Local and diffuse mechanisms of primary afferent depolarization and presynaptic inhibition in the rat spinal cord

Malcolm Lidierth

King's College London, Hodgkin Building, Guy's Hospital Campus, London SE1 1UL, UK

Two types of dorsal root potential (DRP) were found in the spinal cord of urethane-anaesthetized rats. Local DRPs with short latency-to-onset were evoked on roots close to the point of entry of an afferent volley. Diffuse DRPs with a longer latency-to-onset were seen on more distant roots up to 17 segments from the volley entry zone. The switch to long latency-to-onset occurred abruptly as a function of distance along the cord and could not be explained by conduction delays within the dorsal columns. Long-latency DRPs were also present and superimposed on the short-latency DRPs on nearby roots. Both local and diffuse DRPs were evoked by light mechanical stimuli: von Frey hair thresholds were ≤ 1 gram force Changes in excitability of the terminals of sural nerve afferents were used to confirm that both local and diffuse DRPs were associated with primary afferent depolarization (PAD). These effects were potent: the area of the antidromic volley evoked in the sural nerve by intraspinal microstimulation in the L4/5 spinal segment was increased by 109 $\pm$ 50% (mean $\pm$ S.D.; $n = 5$) by nearby conditioning stimuli, and by 52 $\pm$ 12% ($n = 6$) with stimuli applied 9–13 mm (5–8 segments) away. The time course of the changes in terminal excitability closely matched those of the DRPs. Reduction of the field potentials evoked in the dorsal horn by stimulation of dorsal roots was also shown to accompany both local and diffuse DRPs. The area of the monosynaptically evoked field potential was reduced by 48 $\pm$ 19% ($n = 7$) with nearby conditioning stimulation and 16 $\pm$ 9% ($n = 10$) with stimulation 9–12 mm distant. Evidence is presented that this inhibition includes a presynaptic component. Similar effects were seen with field potentials evoked by sural nerve stimulation. It is concluded that diffuse DRPs are mediated through propriospinal networks which may contribute to the gating of sensory information flow during natural behaviour as they respond to weak mechanical stimuli and provoke presynaptic inhibition.

(Received 30 March 2006; accepted after revision 20 July 2006; first published online 27 July 2006)
Corresponding author M. Lidierth: King's College London, Hodgkin Building, Guy's Hospital Campus, London SE1 1UL, UK. Email: malcolm.lidierth@kcl.ac.uk

Presynaptic inhibition of the effects of primary afferents on their spinal targets provides a mechanism by which information flow through the central nervous system may be regulated at the first central synapse. Inhibition of this type is thought to contribute to the regulation of both spinal reflex and ascending pathways (reviewed in Rudomin & Schmidt, 1999). It is strongly implicated as a major mechanism underlying the dynamic regulation of the distribution and size of the receptive fields of spinal neurones (Wall, 1995; Wall *et al.* 1999) and in movement-related gating of sensory transmission (e.g. Cote & Gossard, 2003; Menard *et al.* 2002; Seki *et al.* 2003).

The most studied form of presynaptic inhibition of primary afferents is that associated with primary afferent depolarization (PAD) of the afferent terminals (reviewed in Rudomin & Schmidt, 1999; Willis, 1999). Among Group I muscle afferents, the circuits underling PAD are precisely organized with three types of PAD being recognized on the basis of the pattern of convergence and sign-of-effect of inputs from skin and muscle, and from descending pathways (Rudomin & Schmidt, 1999). Rather less is known about the circuits regulating PAD in cutaneous afferents. However, a general principle appears to be that afferents of one modality most strongly influence those of the same modality. The specificity extends to subclasses of afferents which most strongly inhibit afferents of their own subclass, e.g. slowly adapting mechanoreceptors are most strongly depolarized by other slowly adapting mechanoreceptors (Schmidt, 1971; Whitehorn & Burgess, 1973).

In addition to the modality specificity, there is specificity in the spatial organization of PAD. The last-order

 DOI: 10.1113/jphysiol.2006.110577

interneurones mediating PAD have been shown to operate over short distances in the spinal cord: for interneurones mediating PAD in cutaneous and Group II muscle afferents in the pudendal nucleus of the cat sacral cord, this distance is as short as 2 mm (Jankowska *et al.* 2000). Differential regulation of the terminals of single muscle afferents in different spinal segments has been demonstrated (Eguibar *et al.* 1994; Lomeli *et al.* 1998, 2000) and it has also been shown that individual terminals within a single spinal segment can be differentially regulated (Eguibar *et al.* 1997).

Several early studies suggest that the modality and spatially specific pathways described above operate in parallel with a more diffuse mechanism. These studies have all used recordings of the dorsal root potentials (DRPs) that arise as a consequence of PAD (Barron & Matthews, 1938) to monitor its spinal distribution. In the toad, Dun & Feng (1944) showed that stimulation of a dorsal root could evoke DRPs on roots lying several segments rostral to the stimulus. This is also the case in the cat (Devor *et al.* 1977; Lupa *et al.* 1979). With stimulation of peripheral cutaneous nerves in the cat, Carpenter *et al.* (1963) identified two components to the DRP which they labelled Components I and II. Component I had a restricted rostrocaudal distribution, was present in decerebrate animals both before and after spinal transection and had a short latency-to-onset. In contrast, Component II was diffusely distributed over a wide rostrocaudal extent. It had a long latency-to-onset and, in the decerebrate cats, was present only after spinal transection. Later, Mallart (1965) showed that DRPs could be evoked on lumbar roots by forelimb stimulation in cats under chloralose anaesthesia and with intact neuraxes. More recently, intersegmental coupling of DRP-generating circuits has been demonstrated from recordings of spontaneous DRPs which, in the rat, are temporally synchronized even when recorded from widely separated spinal segments (Lidierth & Wall, 1996; see also Manjarrez *et al.* 2000, 2003).

Despite the reports of their existence, little attempt has been made to examine the diffuse DRPs systematically. For example, it remains to be shown whether the diffuse DRPs accompany active depolarization of the afferent terminals or whether they are associated with inhibition at the primary afferent synapse. This was the purpose of the present study where the diffuse DRPs have been compared with those of more restricted spatial extent and have been characterized more fully.

Some preliminary observations have been reported (Lidierth & Wall, 2001; Lidierth, 2005*a*).

Methods

Experiments were performed on adult male Sprague-Dawley rats anaesthetized with urethane (1.25 g kg^{-1} I.P., supplemented if required). Experimental procedures conformed with, and were licensed under, UK legislation (Animals (Scientific Procedures) Act 1986). At the end of each experiment, animals were killed by an anaesthetic overdose.

The trachea and carotid artery were cannulated, together with the jugular vein in most experiments, and the rat was mounted in a stereotaxic frame providing support via ear bars and pelvic clamps. Rectal temperature was monitored and used to regulate a homeothermic blanket. The electrocardiogram was recorded via percutaneous electrodes in the right and left forelimbs.

A laminectomy was made to expose the spinal cord from the thoracic level to the cauda equina. In most experiments the cord was transected at mid-thoracic level. Where required, the sural nerve was exposed from the calf to the popliteal fossa. Skin flaps and muscle around the exposure were raised and tied to form a pool, which was filled with warm paraffin to protect the exposed cord or nerve.

For recording, gallamine triethiodide (20 mg I.V. or i.a) was administered to achieve neuromuscular blockade and the rat was artificially ventilated. Expired CO_2 was monitored, and ventilation volume adjusted, to maintain an end-tidal CO_2 concentration of 3–4%.

Recording

Dorsal roots were cut and mounted across pairs of Ag–AgCl wires to record dorsal root potentials (DRPs, Fig. 1*A*). Where required, a chloridized silver ball electrode or tungsten-in-glass microelectrode on the cord surface was used to record the cord dorsum potential (CDP, Fig. 1*A*) and was referenced to an electrode in nearby muscle. Analog recordings were amplified and filtered prior to digitization. Low cut-off filter frequencies were no higher than 0.5 Hz (−3dB). When fast components of the DRPs or CDPs were examined, high cut filters were set to 5 kHz. Otherwise cut-off frequencies of 1500 Hz were used.

Antidromic compound action potentials were recorded from the cut ends of the sural nerve which was exposed in the periphery (Fig. 5*A*). The cut nerve was placed across a pair of Ag–AgCl wires with the distal electrode on the crushed end to yield a monophasic action potential (see Wall, 1958). Recordings were filtered (bandpass of 0.5–5000 Hz or higher). The intraspinal terminals of primary afferent fibres were stimulated via a tungsten-in-glass microelectrode.

Dorsal horn field potential recordings were made with tungsten-in-glass microelectrodes (Fig. 7*A*). Electrodes were positioned on the dorsal horn to optimize the antidromic volley and its modulation by conditioning stimuli applied to a nearby dorsal root (see Results). Recordings were buffered by a high input-impedance headstage prior to amplification and filtering (bandpass of 0.5–5000 Hz or higher).

Stimulation

Dorsal roots and peripheral nerves were cut and mounted across two Ag–AgCl wires for electrical stimulation (Figs 1*A*, 5*A* and 7*A*). Stimuli were of 200 μs duration and were delivered every second. In some experiments, fixed currents of 10 or 100 μA were used. In others, the threshold for the most excitable afferents was determined from the CDP at the spinal entry of the stimulated root or nerve, or by recording the volley from the intact root proximal to the stimulus. Stimulus strengths were then expressed as multiples of this threshold ($\times T$).

In all cases, stimuli were delivered from an isolated constant current source (Neurolog NL800 or Grass SIU7) and were monitored by recording the voltage drop across a resistor placed in the current return path. Pulse sequences were generated using a stand-alone timing device (D4030, Digitimer UK) or Pulser software (Lidierth, 2005*b*).

Data analysis

All recordings were digitized and averaged using a PC and interface card (1401plus or micro1401 MkII) with Signal or Spike2 for Windows software (Cambridge Electronic Design, Cambridge, UK). On-line and preliminary analysis of the data were also performed in these software environments. Filtered signals were digitized at a sample rate not less that 3 times the high frequency filter cut-off.

To examine the time course of the effects of conditioning stimuli, condition-test (C-T) stimulus pairs and control stimuli (test alone) were delivered alternately. For examining the effects of conditioning stimuli on the dorsal horn field potentials evoked by dorsal root or sural nerve stimuli, C-T pairs, control stimuli and conditioning stimuli alone were delivered cyclically. The averaged responses evoked by the conditioning stimulus when delivered alone were digitally subtracted from the test average. The interval between conditioning and test stimuli was varied to examine the time course of the effects of conditioning. As has been noted elsewhere (e.g. Eccles *et al.* 1962*a*), the effects of a preceding test stimulus can depress the recorded potentials when short interstimulus intervals are used. The decision to use a 1 s interval here was a compromise which allowed many C-T curves to be constructed for each preparation while keeping the effects of any residual depression to a minimum. The introduction of a conditioning stimulus only period when examining field potentials (see above) meant that the test stimuli in the C-T pair and control periods were not evenly spaced and therefore not always equally affected by the residual depression. Control responses could be underestimated, typically being ~98% of the expected value. To control for this affect, a baseline period was examined in which the test stimuli were delivered prior to the conditioning stimulus (i.e. negative C-T stimulus intervals were used, e.g. −40 to −5 ms in Fig. 6). The reduction of the control response meant that test–response amplitudes could be elevated above the expected 100% of control over the baseline period (see, e.g. Figs 7*F* and 10). To accommodate these affects, changes in the responses were judged significant only if they fell outside of two standard deviations of the mean value over the baseline period and the size of the effects was expressed as a 'modulation depth' calculated

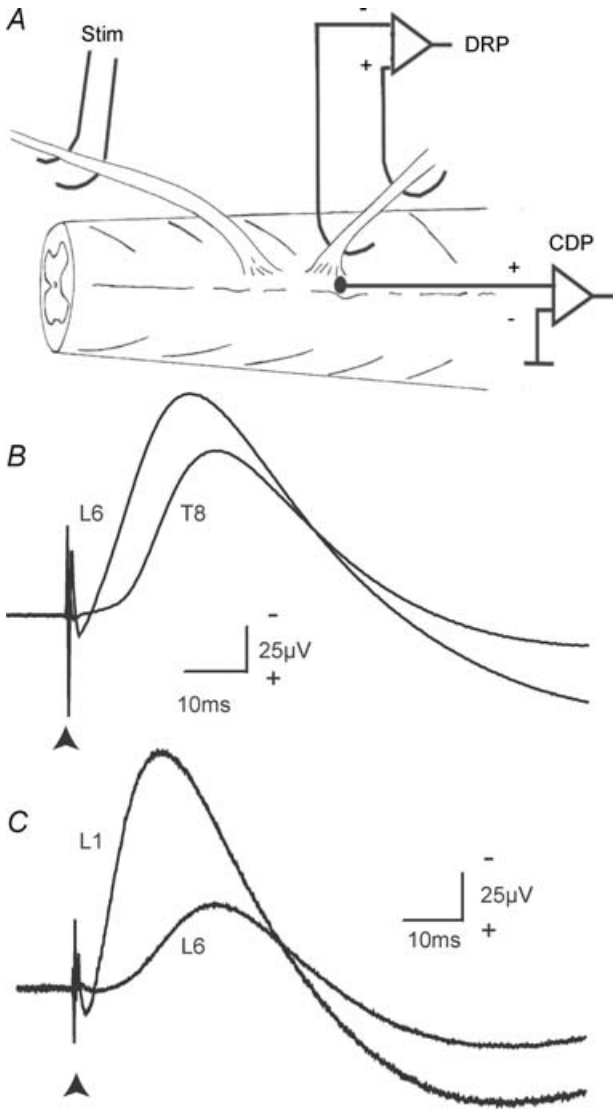

Figure 1. Near and distant DRPs
A, the experimental arrangement for stimulating dorsal roots and recording the DRP and CDP. By convention (Barron & Matthews, 1938), the proximal electrode is connected to the inverting input of the amplifier and DRPs are illustrated negative-up. Typical DRPs are shown in *B* and *C*. *B,* a stimulus to the L5 root (10 μA; 200 μs pulse) evoked a DRP on the nearby L6 dorsal root (2 mm) and also on the more distant T8 root located 17 mm away. The arrowhead marks the time of the stimulus. The spinal cord had been transected at mid-thoracic level in this animal. *C*, similar potentials from a preparation with an intact spinal cord. The stimulus was to the T13 dorsal root and recordings were made at L1 (distance 2.5 mm) and L6 (11.5 mm).

as the difference between the baseline mean and the minimum value at positive C-T intervals (or maximum value where appropriate).

Results

DRPs on distant roots

Figure 1*B* shows averaged DRPs recorded simultaneously from the L6 and T8 dorsal roots and evoked by electrical stimulation of an L5 rootlet. The stimulus evoked a pronounced DRP not only on the nearby L6 root, which had its dorsal root entry zone (DREZ) located 2 mm caudal to that of the stimulated rootlet, but also on the more distant T8 root located 17 mm rostrally. Both DRPs were of large amplitude and long duration: 122 μV and 56 ms on L6 compared with 90 μV and 54 ms on T8. However, the latency to onset of the DRP on the L6 root was short at 2.2 ms while that for the T8 DRP was comparatively long at 8.1 ms for the sharply rising (negative) phase judged from a differentiated trace. The peak of the DRPs occurred at 21.2 ms on L6 and 26.2 ms on T8. Note that the spinal cord had been transected at mid-thoracic level in this animal thus interrupting all long-loop pathways. However, similar DRPs were present in preparations with intact neuraxes, as shown in the examples of Fig. 1*C*.

For the traces of Fig. 2*A*, a stimulus was delivered to the third coccygeal (Co3) root and recordings were made from more rostral dorsal roots or divided rootlets as far rostral as T10. For this purpose DRPs were recorded from one root at a time, the recording electrodes being moved successively from the T10 dorsal root to Co2. DRPs on the most closely neighbouring roots, up to the S2 level were of short latency: 2.3 ms on Co2, 2.8 ms on Co1, 3.6 ms on S3 and 3.7 ms on S2 (S4 was not recorded from in this animal). The rate of rise of the DRPs exhibited a progressive decline with distance and the peaks showed a progressive increase in latency occurring at 12.1 ms, 18.5 ms, 28.5 ms and 31.3 ms, respectively. The DRPs exhibited a sharp transition to a delayed onset at the S1 level where the DRP had a latency-to-onset of 10.9 ms. On more rostral roots, delayed-onset DRPs were also present but, in this example, there was no apparent systematic increase in latency rostral to S1: for the 14 roots or rootlets recorded between the S1 and T10 levels, the latency was 10.4 ± 1.2 ms (mean $\pm$ S.D.).

A similarly abrupt change in latency-to-onset with distance was observed when DRPs were recorded from roots located caudal to the stimulus as shown in Fig. 2*B* where stimuli were delivered to the T10 dorsal root and DRPs were recorded successively from roots or rootlets between T11 and Co3 levels. On the nearby roots, short-latency DRPs were present with latencies-to-onset of 1.8 ms on T11 and 3.4 ms on T12 and T13. At L1, a transition occurred such that the most prominent component of the DRP had a longer latency-to-onset although short-latency components of low-amplitude were present on some more caudal traces, e.g. L6 and S1.

In the traces of Fig. 2*B*, there was a clear trend in which the latency of the delayed DRPs increased as recordings were made from successively more caudal roots: a least-squares regression through for the latency-to-onset of the DRPs for L1 through Co3 provided a regression line with an intercept of 5.7 ms and a slope of 0.23 ms mm^{-1} ($R^2 = 0.74$; $n = 15$). The 95% confidence intervals on the slope of this line corresponded to velocities of propagation along the spinal cord of 3.2–6.8 m s^{-1}.

Form of the potentials

With a stimulus to a nearby dorsal root, the prolonged negative DRPs described above were accompanied by a series of four earlier potentials. Similar potentials, and their origins, have been described in the cat where they were labelled DR I to DR IV while the prolonged negative potential was labelled DR V (Lloyd & McIntyre, 1949). Each of these potentials is present also in the rat (Wall & Lidierth, 1997).

Figure 2*C* and *D* illustrates, at slow and fast time bases, respectively, the averaged DRPs (black lines) and CDPs (grey lines) recorded at L3 level following stimulation of more caudal roots. With stimulation of the nearby L4 root, an initial negative–positive–negative complex includes components DR I, II and III (as indicated in Fig. 2*D*). This complex was coincident with the arrival of the afferent volley recorded from the nearby cord dorsum and marked 'Vol' in Fig. 2*D*. When stimuli were delivered to roots at greater distance from the recording point, the afferent volley was still apparent in the CDP and was coincident with a complex in the DRP, but this complex took a variable form. A short negative potential generally dominated but could be part of a mono-, bi- or triphasic complex. Examples are shown in Fig. 2*C* and *D* where recordings were made at L3 level and stimuli were delivered to the dorsal roots of the L6 and S3 segments. In the illustrated cases, the afferent volley seen on the CDP was accompanied by a negative component with L6 root stimulation and a biphasic, negative–positive, complex with S3 stimulation (marked with an asterisk in Fig. 2*D*).

At short distances, the prolonged negative DRP, was preceded by a period of positivity (DR IV of Lloyd & McIntyre, 1949). This overlapped in time with a negative (N) wave in the CDP (Fig. 2*D*). At greater interroot distances DR IV was absent, as was the N-wave of the CDP (e.g. with S3 root stimulation in Fig. 2*D*), and DR V arose at long latency from a steady baseline. At both short and long distances, DR V was accompanied by a positive (P) wave on the CDP (Fig. 2*C* and *D*). With distant stimuli, the onset of the P-wave invariably preceded the onset of DR V

(as with L6 and S3 stimulation in Fig. 2*D*). At intermediate stimulation distances, the P-wave could be biphasic (as with L6 stimulation in Fig. 2*C*).

The early triphasic complex (DR I–III) was also seen in the experiment illustrated in Fig. 2*A*, where DRPs were recorded at various levels of the spinal cord (their absence in Fig. 2*B* is because the high cut filter frequency was lower). The early complex propagated in strictly linear fashion along the cord: for the examples in Fig. 2*A*, the velocity of propagation was 26–28 m s^{-1} (95% confidence limits on slope from least squares regression; $R^2 = 0.99$, $n = 18$). Note that the abrupt change in latency-to-onset of the prolonged negative DRP was not associated with any discontinuity in the velocity of propagation of the early volley.

DRPs evoked by natural stimulation

The DRPs evoked in response to light mechanical stimulation of the central pad of the ipsilateral

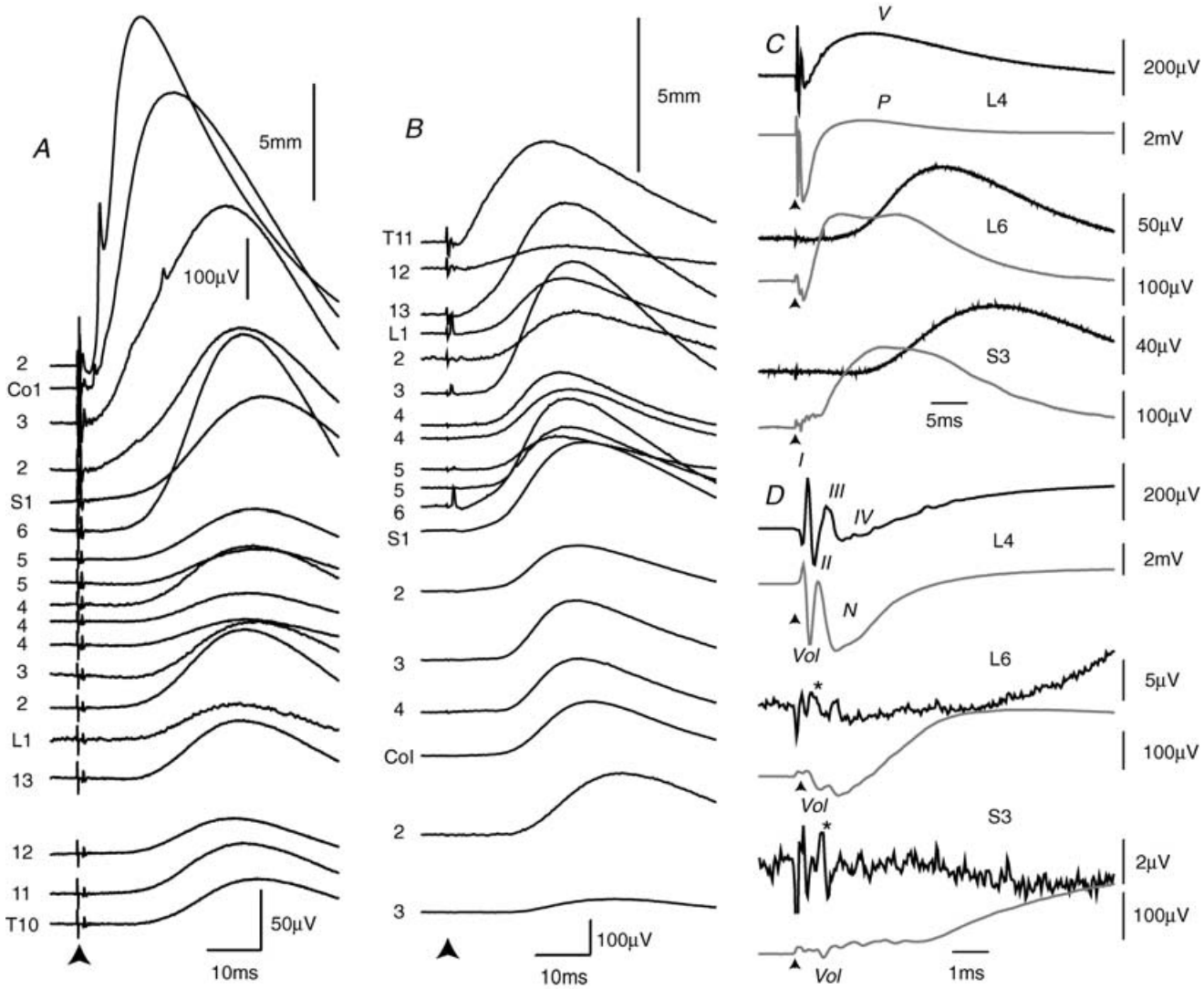

Figure 2. Effect of distance on the latency and form of the DRP
A, averaged DRPs evoked by a stimulus to the third coccygeal dorsal root (Co3) and recorded on successively more rostral dorsal roots, or divided rootlets, up to the T10 spinal level in a single animal. Each trace has been positioned so that the vertical displacement of the prestimulus period is proportional to distance along the cord (5 mm calibration bar shown; note that the voltage calibration is different for the upper 3 traces). *B*, as in *A*, but from another preparation in which the T11 dorsal root was stimulated and DRPs were recorded from successively more caudal roots. *C* and *D*, averaged DRPs (black lines) and CDPs (grey lines) evoked at the L3 level in response to stimulation of more caudal dorsal roots (L4, 0.5 mm separation; L6 5.5 mm and S3, 11 mm). The traces are shown on a slow time base in *C* and a fast time base in *D*. Stimuli were 10 μA, 200 μs pulses in all cases. Traces in *C* and *D* are from a single animal.

hindpaw with a von Frey hair were examined in three rats. In these animals, the caudal part (∼1/3rd) of the L5 dorsal root was teased free and mounted for recording of the DRP, the remainder of the root being left in continuity. A thoracic DRP (T10–T13) was recorded simultaneously. DRPs were reliably evoked on both L5 and thoracic roots by forces of 1 gram force (< 0.01 N). Responses to lower strength stimuli appeared to be present but could not be discriminated reliably from the background activity of spontaneous DRPs (see Lidierth & Wall, 1996).

In 10 rats, prepared as above, the DRPs evoked by a brisk non-noxious tap to the plantar surface of the hindpaw were recorded simultaneously from the L5 root and from a thoracic dorsal root (T9–T12). Example DRPs evoked in response to five successive paw taps in one animal are shown superimposed in Fig. 3*A*. The DRP at T12 was clearly delayed compared to that at L5. To quantify this delay, the peaks of the L5 DRPs were discriminated in software and used to trigger averages of the recordings. Specimen averages are shown to the left in Fig. 3*B*. Across the 10 rats, the delay to the peak of the DRP on the thoracic root was longer than that on the L5 root by 8.3 ± 5.3 ms (mean ± s.d.).

When the DRPs evoked by a tap to the paw had been recorded in each of the 10 rats described above, the L6 root was cut and mounted for electrical stimulation and the electrically evoked DRPs were averaged. Specimen traces are shown to the right in Fig. 3*B*. The delay to the peak of the electrically evoked DRP on thoracic roots was 9.5 ± 3.4 ms (mean ± s.d., $n = 10$) longer than that on the L5 root.

Figure 3*C* compares the latencies of the DRPs evoked by electrical and by paw-tap stimuli in each animal. For 8 of the 10 rats, the difference in latency between the peaks of the DRPs on L5 and thoracic roots was greater with electrical stimulation than with mechanical stimulation. However, the differences were not statistically significant ($P > 0.05$; Signed ranks test, $n = 10$).

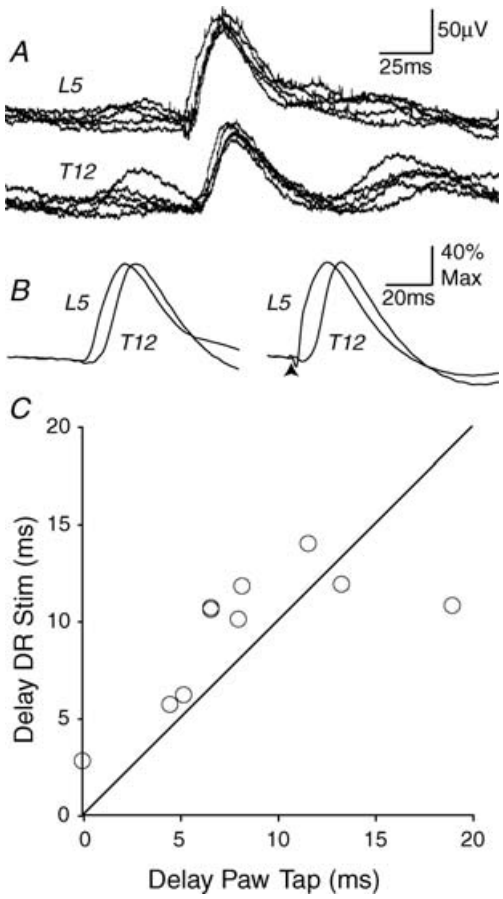

Figure 3. Comparison of mechanically and electrically evoked DRPs

A, the DRPs evoked at L5 and T12 levels by five successive taps to the plantar surface of the ipsilateral hindpaw with a blunt probe. *B,* shows the averaged response to the paw tap (left; 22 stimuli) together with that evoked by an electrical stimulus to the L6 dorsal root (right; 10 μA, 200 μs stimulus, 43 stimuli). The traces in *B* have been scaled to equal heights to assist comparison of the timecourses. Data are from a single preparation. In *C*, the delays between the peaks of the DRP on thoracic roots (T9–T12) and those on L5 roots are plotted for 10 animals. The line in *C* is the line of equality.

Effects of the $GABA_A$ antagonist picrotoxin

Systemic administration of picrotoxin produced a dose-dependent reduction in the amplitude of the DRPs evoked on both nearby and distant dorsal roots. Figure 4*A* illustrates the results for one animal. DRPs were averaged across 30 stimulus presentations and their amplitudes were plotted as a function of time. A dose of 2 mg kg^{-1} picrotoxin reduced the amplitude of the evoked DRPs to 83% and 80% of control on the L5 and T11 roots, respectively. The effects of picrotoxin were prolonged. Successive doses were therefore assumed to have additive effects and dose–response relations were calculated using the cumulative dose. Progressively higher cumulative doses of picrotoxin produced progressive reductions in the amplitude of both DRPs but they were not abolished: at 100 mg kg^{-1} picrotoxin, the L5 DRP was 18% of control amplitude while that for T11 was 17% of control amplitude.

Pooled dose–response data for the effects of picrotoxin in four animals are shown in Fig. 4*B* at cumulative doses of 2–100 mg kg^{-1}. The picrotoxin-resistant component of the DRP, estimated from the minima of the Hill plots fitted in Fig. 4*B*, had amplitudes of 16.7 and 16.3% of control for L5 and T11 DRPs, respectively.

Changes in terminal excitability accompanying the DRPs

The changes in excitability of afferent terminals to stimulation of nearby and distant roots were examined to

establish whether the distant DRPs were associated with changes in excitability of the terminals consistent with PAD. Microstimuli ($< 10\mu$A) were delivered through a microelectrode which was advanced into the spinal cord just medial to the dorsal root entry zone at the L5 (or caudal L4) level while recording the antidromic compound action potential monophasically from the sural nerve (Fig. 5*A*). A substantial antidromic volley was evoked when the stimulating electrode was close to the cord surface. The amplitude of this volley declined as the electrode was advanced but grew again as the electrode tip entered the region of the afferent terminals in the deep dorsal horn (450–550 μm deep). With the electrode at this depth, the test-stimulus was adjusted (1) to evoke a reliable antidromic volley and (2) so that the evoked volley exhibited a clear increase in size when preceded by a conditioning stimulus to a nearby dorsal root. The time course of the effects of a conditioning stimulus to more distant roots was then examined.

Antidromic volleys recorded from the sural nerve in one preparation are illustrated in Fig. 5*B* where control (grey lines) and test (black lines) responses are shown superimposed. When conditioning stimuli were applied, the antidromic volleys increased in size and there was a corresponding increase in their area. The time course of these effects is illustrated more fully in Fig. 5*C* with data from another preparation in which conditioning stimuli were applied to dorsal roots of segments located both rostral and caudal to the test stimulus at L5. Responses are shown with conditioning test-stimulus intervals of 0–50 ms as indicated together with the two control responses (Con) that were recorded concurrently with the test responses at C-T stimulus intervals of 0 and 50 ms. Elevation of the size of the antidromic volley in response to conditioning stimulation of each root is apparent. With interstimulus intervals of 10 ms, the responses were significantly elevated (i.e. ≥ 2 S.D. above baseline) with conditioning stimulation of the nearby L3 and L6 roots and, in this preparation, also the more distant L1 root. For the remaining roots, significant elevation of the response was absent at 10 ms but present at 20 ms interstimulus intervals. Responses remained significantly elevated with interstimulus intervals of 45 ms or more in all cases.

To quantify the changes in excitability, the areas of the averaged compound action potentials were measured and the C-T stimulus interval was varied to permit the time course of the changes to be examined. The area of the initial monophasic component was measured in software. Test stimuli delivered alone (control) were alternated with those preceded by a conditioning stimulus. Control responses were averaged and the area of the test responses were expressed as a percentage of the mean control area ($\pm$ S.D.) for each interval tested. Figure 6*A* shows the resulting time courses for one animal in which conditioning stimuli were delivered to the S1 and L2 dorsal roots (2 mm caudal and 4 mm rostral to the test electrode, respectively) and to the S2 and T12 roots (7 mm caudal and 9.5 rostral). Conditioning stimulation of the nearby S1 and L2 roots was followed by an increase in the area of the test response with a latency-to-onset of 3 and 4 ms, respectively (i.e. at these latencies, the area exceeded the baseline mean by 2 standard deviations or more). The antidromic volley recorded from the sural nerve remained elevated with stimuli of up to 100 ms separation in both cases. For the more distant roots, the onset of change in terminal excitability was of longer latency: 8 ms with T12 and 14 ms with S2 root stimulation. As with conditioning

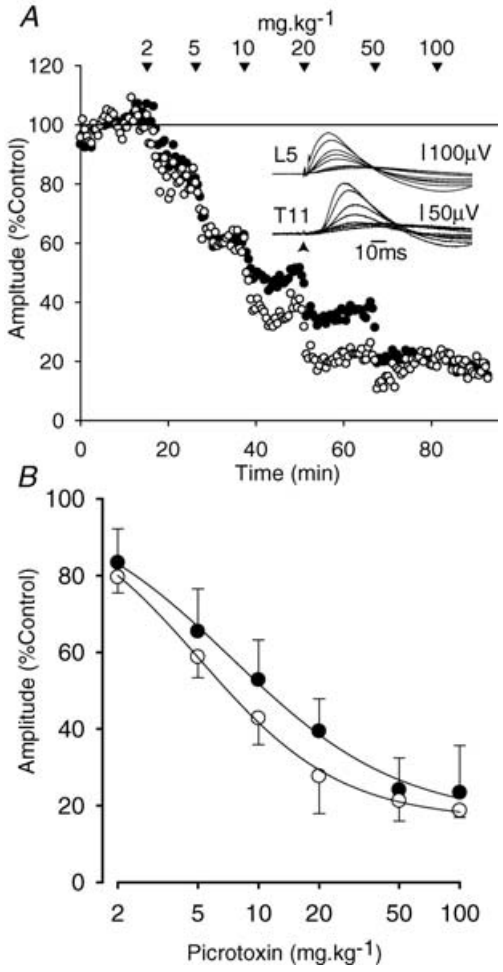

Figure 4. The effects of picrotoxin on the amplitude of the DRP
A, the data from a single experiment in which the L6 dorsal root was stimulated at 100 $\times$ *T* while recording the DRPs at the L5 (●) and T11 (○) levels. DRPs were averaged over 30 stimuli and their amplitudes are plotted as a function of time. Picrotoxin was administered intravenously at the times indicated. Doses are cumulative. The insets show specimen averaged traces for each dose together with a control trace. *B*, the pooled results from five animals (three animals where both L5 and T11 DRPs were successfully recorded over the course of the experiment and two others in which only one of the L5 or T11 DRPs was recorded throughout). Data shown are means $\pm$ S.D. ($n = 4$ for doses of 2–50 mg kg^{-1}, $n = 3$ for 100 mg kg^{-1}).

stimulation of nearby roots, this increase in area was of long duration.

When the time course of the changes in excitability had been determined, a component of the L5 dorsal root close to the test electrode was teased free and mounted for recording of the DRP. The DRPs evoked by each of the conditioning stimuli were then recorded and averaged and are shown above each graph in Fig. 6*A*. It is clear that the time course of the increase in area of the antidromic volleys in the sural nerve closely resembled the time course of the prolonged negative DRPs.

Graphs such as those of Fig. 6*A* were constructed with conditioning stimulation of 26 dorsal roots in six rats. The results are summarized in Fig. 6*B* and *C*. In Fig. 6*B*, the modulation depth (i.e. the difference between the peak area and the baseline mean) is plotted as a function of distance from the test stimulus site. While modulation depth decreased with distance, strong modulation was still apparent even when conditioning stimuli were applied up to 13 mm from the test site. The area of the antidromic volleys was increased by $109 \pm 50\%$ (mean $\pm$ S.D.; $n = 5$) by conditioning stimuli located 0–3 mm from the test stimulus site, and by $52 \pm 12\%$ ($n = 6$) with stimuli applied 9–12 mm (5–8 segments) away.

In Fig. 6*C*, data have been pooled according to the distance between the conditioned dorsal root and the test stimulus site. At distances of 0–3 mm, conditioning stimuli produced a significant rise in terminal excitability with a latency-to-onset of 2 ms as judged from the area of the antidromic volley. The latency-to-onset increased with distance: to 4 ms at 3–6 mm and 8 ms at 6–9 and 9–12 mm. The latency to the peak effect also increased with distance

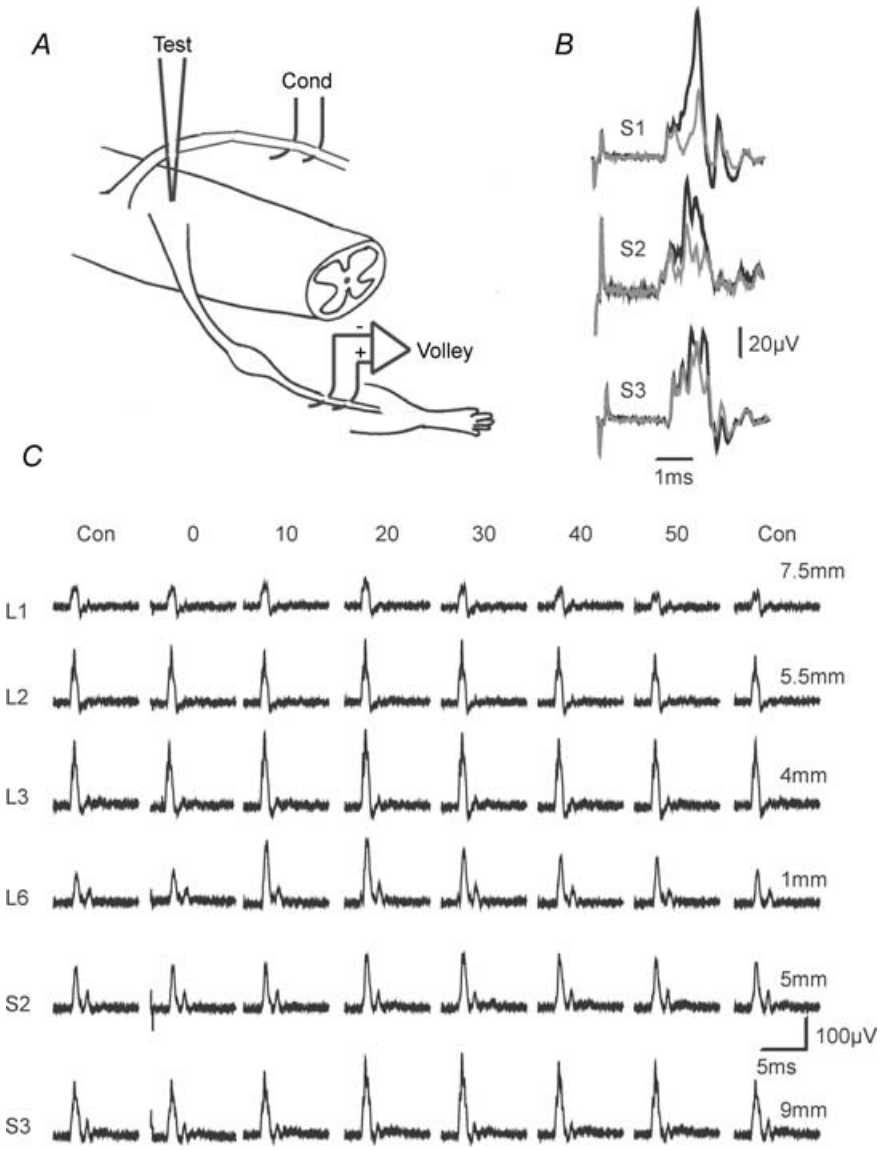

Figure 5. Changes in excitability of sural nerve terminals
A, the experimental arrangement. *B,* specimen averaged antidromic volleys recorded from the sural nerve. The effects of conditioning stimuli of 100 μA strength were examined when applied to the S1, S2 or S3 roots. Test stimuli were of 6.0, 8.4 and 6.0 μA, respectively, and were delivered to the dorsal horn in the L5 segment (for conditioning stimulation of S1 and S3 roots) or at the L4/5 boundary (S2) at interstimulus intervals of 14 ms (S1) or 22 ms (S2 and 3). Control (grey) and test (black) responses are superimposed. *C*, the time course of this effect with stimulation of roots located rostral to the test stimulus (L1, distance 7.5 mm; L2, 5.5 mm and L3, 4 mm) and caudal (L6, 1 mm; S2, 5 mm and S3, 9 mm). Data are from a single experiment.

although the size of the peak exhibited a general decline with distance: 16 ms at 0–3 mm (modulation depth from Fig. 6*C* of 97%), 18 ms at 3–6 m (50%), 22 ms at 6–9 mm (67%) and 24 ms at 9–13 mm distance (43%).

Inhibitory effects on primary afferent-evoked field potentials in the dorsal horn

The effects of conditioning stimulation on the responses evoked in the dorsal horn of the spinal cord by electrical

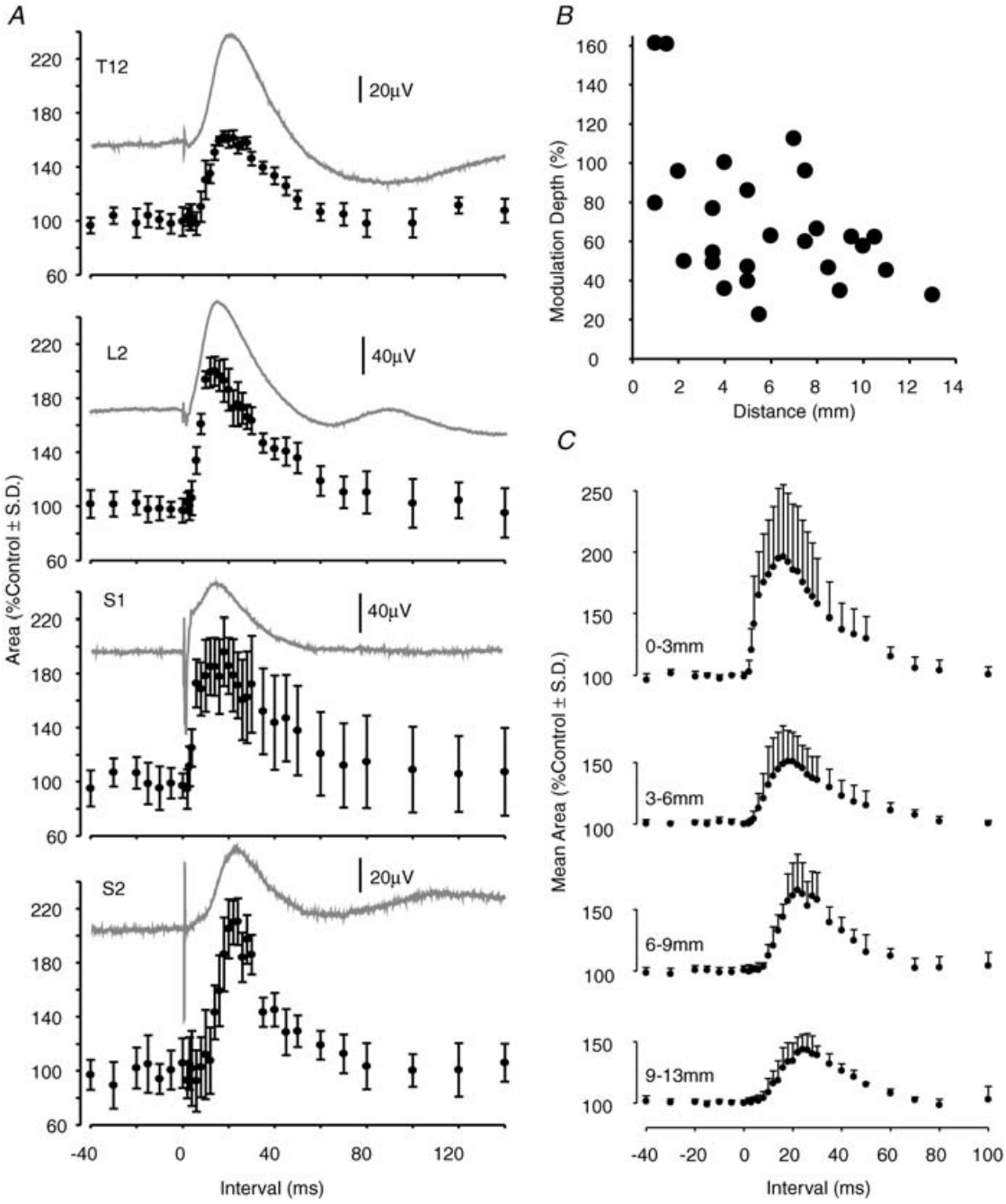

Figure 6. Magnitude and time course of the changes in excitability of sural nerve terminals
A, a quantitative analysis of the data from an experiment in which conditioning stimuli were applied to the T12, L2, S1 or S2 dorsal roots (distances from the test-stimulus site of 9.5, 4, 2 and 7 mm, respectively). Test stimuli in the L5 segment were 4.3–6.4 μA. Conditioning stimuli were 100 μA in all cases. The DRPs recorded subsequently with stimulation of each conditioning root are superimposed on the graphs. *B* and *C*, summarize the data from experiments where graphs such as those shown in *A* were constructed with conditioning stimulation of 26 roots at various distances from the test-stimulation site. *B*, the depth of modulation (see Methods) as a function of distance for each of the 26 roots. *C*, data were pooled to allow an average time course to be calculated for samples where the conditioning root was 0–3 mm distant ($n = 5$), 3–6 mm ($n = 9$), 6–9 mm ($n = 6$) or 9–13 mm ($n = 6$).

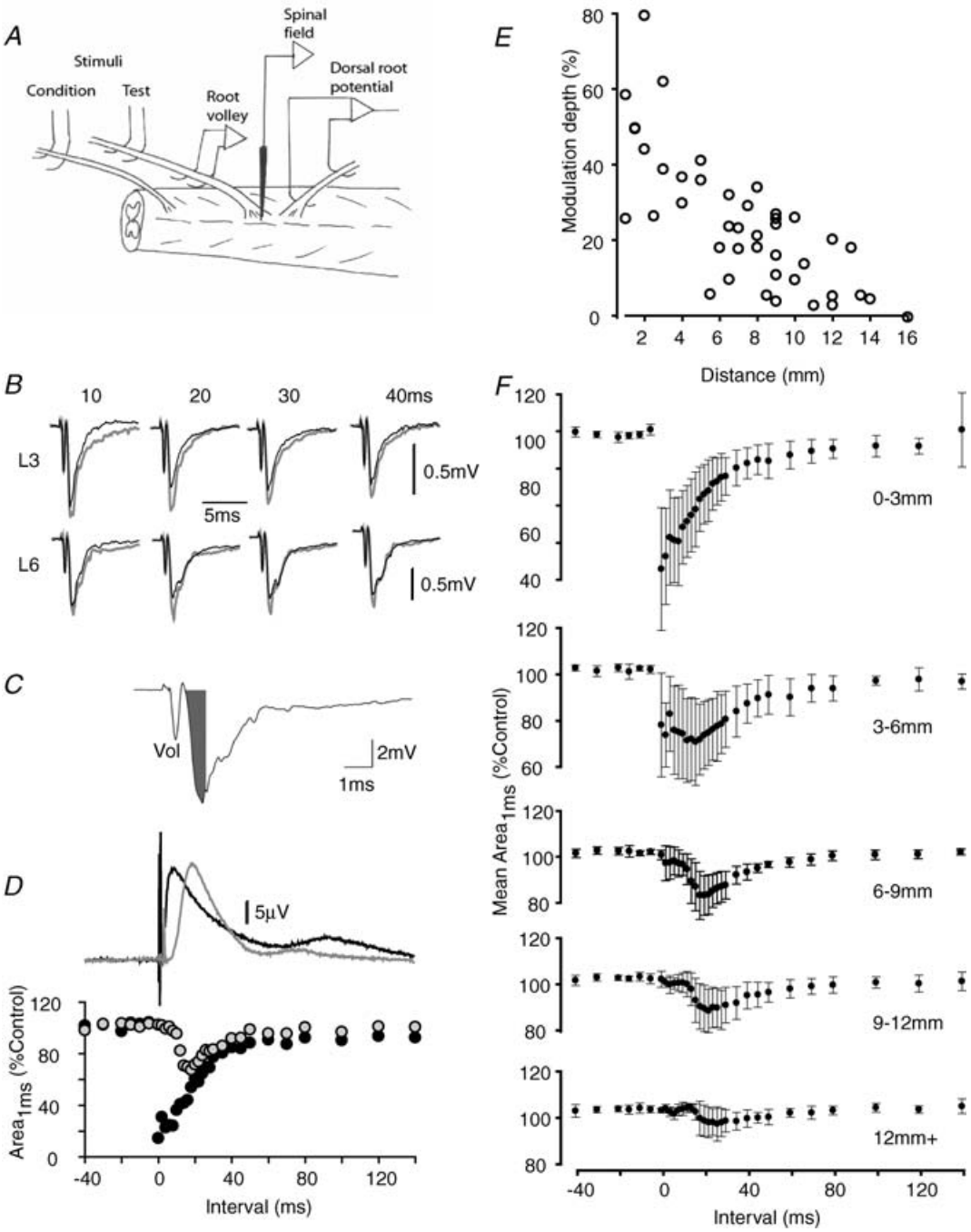

Figure 7. Effects of conditioning stimuli on dorsal root-evoked field potentials in the dorsal horn
A, the experimental setup. *B*, the responses recorded at depth in the dorsal horn of L1 following electrical stimulation of the L1 dorsal root. Control traces are shown (grey lines), together with traces (black lines) that were conditioned by preceding stimulation of the dorsal roots of L3 (upper traces; 4 mm distant) and L6 (lower traces; 10 mm distant) at intervals of 10–40 ms as indicated. *C* shows how the monosynaptic component of the evoked field potential was estimated. The grey filled area ($Area_{1ms}$) covers the negative component of the field up to 1 ms after the peak of the afferent volley recorded at depth ('Vol'). *D*, the full time course of the effects of conditioning stimulation on this component of the evoked field potential. Field potentials were recorded in the L2 dorsal horn and evoked by L2 dorsal root stimulation. Conditioning stimuli were delivered to the dorsal roots of L3 (black circles) or L6 (grey circles) segments and are shown together with the DRPs evoked on the L1 root. Data are from a different preparation to *B*. *E*, the modulation depth measured from graphs such as those in *D*, as a function of distance. Data are from 42 root pairs in 12 animals. *F*, averaged time courses for the inhibition of the monosynaptic component of dorsal horn field potentials calculated from pooled data. Test stimuli (range 0.7–10 μA) were delivered to the dorsal root of the recorded segment and conditioned by stimuli (10 or 100 μA) to dorsal roots with entry zones

stimulation of dorsal roots were examined. Figure 7*A* illustrates the experimental arrangement. Test stimuli were delivered to a cut dorsal root while recording the afferent volley from the same root with a pair of electrodes placed more proximally (or from the cord dorsum in some cases). A microelectrode was advanced into the dorsal horn (400–500 μm depth) to record the responses evoked by the test stimuli. Typical responses are illustrated in Fig. 7*B* and *C*. The response recorded at depth consisted of an initial transient negativity corresponding to the arrival of the afferent volley ('Vol' in Fig. 7*C*) which was followed, after a short delay, by the synaptically evoked focal field potential. The effect on the test response of conditioning stimuli applied to nearby and more distant roots was examined. Note that condition-test (C-T) stimulus pairs, test stimuli alone (control) and conditioning stimuli alone were delivered in sequence, with the sequence being repeated so that test-stimulus evoked responses could be compared with control responses recorded over the same period of recording. The response evoked by the conditioning stimulus delivered alone, was subtracted from the responses evoked by the C-T pairs (as shown in Fig. 8).

Figure 7*B* illustrates these effects at a range of C-T stimulus intervals (10–40 ms as shown) for a test stimulus to the L1 dorsal root which was conditioned by stimuli to the L3 or L6 roots. It is apparent that the size of the evoked field potentials was reduced when conditioning stimuli were delivered to either L3 or L6 dorsal roots and that this inhibition was of prolonged duration. The initial component of the synaptically evoked field potentials must be monosynaptic in origin and thus provides a measure of the effect of the primary afferents on second-order spinal neurons. To isolate the monosynaptic component, the area of the response over the period up to 1 ms after the peak of the afferent volley ($\text{Area}_{1\text{ms}}$) was measured as shown in Fig. 7*C*. Full time courses of the effects from another experiment are shown in Fig. 7*D* (specimen traces for this experiment are shown in Fig. 8).

With conditioning stimulation of nearby dorsal roots, there was commonly a potent inhibition of the monosynaptic field evoked by a test stimulus at very short C-T stimulus intervals which was followed by a partial recovery and then a further prolonged inhibition. In the example of Fig. 7*D*, conditioning stimulation of the L3 dorsal root (black circles), which entered the cord 2 mm caudally to the recording point, produced a pronounced inhibition of the response to stimulation of the L2 dorsal root. With simultaneous presentation of conditioning and test stimuli, the area of the monosynaptic component was reduced to 14% of control. A slight recovery, to 31% of control, occurred when the C-T stimulus interval was increased to 2 ms but the size of the inhibition then increased again, with responses averaging 24% of control for stimulus separations between 4 and 8 ms. This was followed by a gradual decline in the strength of the inhibition with a prolonged time course that was similar to that of the DRP. In Fig. 7*D*, full recovery of responses to control levels was not present even at stimulus intervals of 140 ms, which was the maximum interval tested, and where monosynaptic response areas were 90% of control.

The second trace of Fig. 7*D* (grey circles) shows the effects of delivering a conditioning stimulus to the more distant L6 dorsal root. Inhibition of the monosynaptic component of the synaptic field evoked by stimulation of the L2 dorsal root was present again, but was distinct from that evoked with stimulation of the L3 root in two respects. (1) There was less, or no, inhibition at short C-T stimulus intervals. For the example shown in Fig. 7*D*, responses were not significantly reduced (to less than 2 standard deviations below the baseline mean) at interstimulus intervals of less than 10 ms. This compares with a latency-to-onset for the L6 root evoked DRP recorded at L1 level of 7.5 ms. (2) At its peak, the inhibition was less potent than that seen with stimulation of the L3 root (69% of control at 16 ms stimulus separation).

These effects are quantified further in Fig. 7*E* where, for each of 42 pairs of roots from 12 animals, the depth of modulation was estimated from graphs such as those in Fig. 7*D* as the difference between the mean baseline area (where test stimuli preceded conditioning stimuli by 5–40 ms) and the area during the peak inhibition observed when conditioning stimuli preceded the test stimulus by 4 ms or more (note that this excluded the often potent but transient inhibition that occurred with interstimulus intervals of less than 4 ms when conditioning stimuli were delivered to nearby roots. This early inhibition may include a substantial occlusive component). When conditioning stimuli were applied 0–3 mm from the point of recording, the monosynaptic component of the evoked field potential was reduced by $48 \pm 19\%$ (mean $\pm$ S.D., $n = 7$), $36 \pm 17\%$ between 3 and 6 mm ($n = 7$), $21 \pm 9\%$ between 6 and 9 mm ($n = 11$), $16 \pm 9\%$ between 9 and 12 mm ($n = 9$), falling to $8 \pm 8\%$ at 12 mm and beyond ($n = 7$). The latencies to peak inhibition among these trials (mean $\pm$ S.D.) was: 6.3 ± 1.8 ms (0–3 mm), 12.9 ± 5.5 ms (3–6 mm), 20.5 ± 7.3 ms (6–9 mm), 23.4 ± 8.8 ms (9–12 mm) and 22.6 ± 12.2 ms ($\geq$ 12 mm).

located, from above downwards, 0–3 mm from the recording point ($n = 7$), 3–6 mm ($n = 7$), 6–9 mm ($n = 11$), 9–12 mm ($n = 10$) and more than 12 mm ($n = 7$). Error bars show standard deviations. Data were derived from 12 rats.

The size and time course of the effects described above are illustrated further in Fig. 7*F* where data from all 42 root combinations have been pooled according to distance between the roots receiving test and conditioning stimuli and averaged. The potent early inhibition is clear when conditioning stimuli were delivered to roots whose entry zone was less than 6 mm from the recording site. At greater distances, some inhibition is seen at short latencies but a more marked inhibition is always present with latency-to-onset of 12 ms at 6–9 mm distance, 14 ms at 9–12 mm and 18 ms from 12 to 16 mm.

It remains to be determined whether the inhibition described above results from presynaptic or postsynaptic mechanisms. If changes in postsynaptic conductance contribute to the inhibition, the time course of the declining phase of the field potentials shown in Fig. 7*B* would be expected to be more rapid following conditioning stimulation. In the traces of Fig. 7*B*, there appears to be no change in the time course. However, in Fig. 8*E*, with conditioning stimulation of a nearby root, changes are clear. The effect of the conditioning stimulus on the time course can be seen best in Fig. 8*F* where the peaks of the synaptic potentials have been scaled to be of equal amplitude. As the interval between conditioning and test stimuli was increased, the decline of the fields approached a more complete overlap (Fig. 8*F*, 30 and 40 ms). There is evidence, therefore, that stimulation of nearby roots can evoke a postsynaptic conductance change of short duration (∼30 ms; Fig. 8*F*) but these were not always present (Fig. 7*B*). Note that, at short C-T intervals, these conductance changes might include an occlusive interaction between conditioning and test stimuli. In this case, non-algebraic summation of the conditioning and test responses may occur and the process of subtracting away the response to conditioning stimulation to reveal the test response would be less appropriate.

In contrast, when conditioning stimuli were delivered to a more distant root (L6: Fig. 8*L*) the initial declining phase

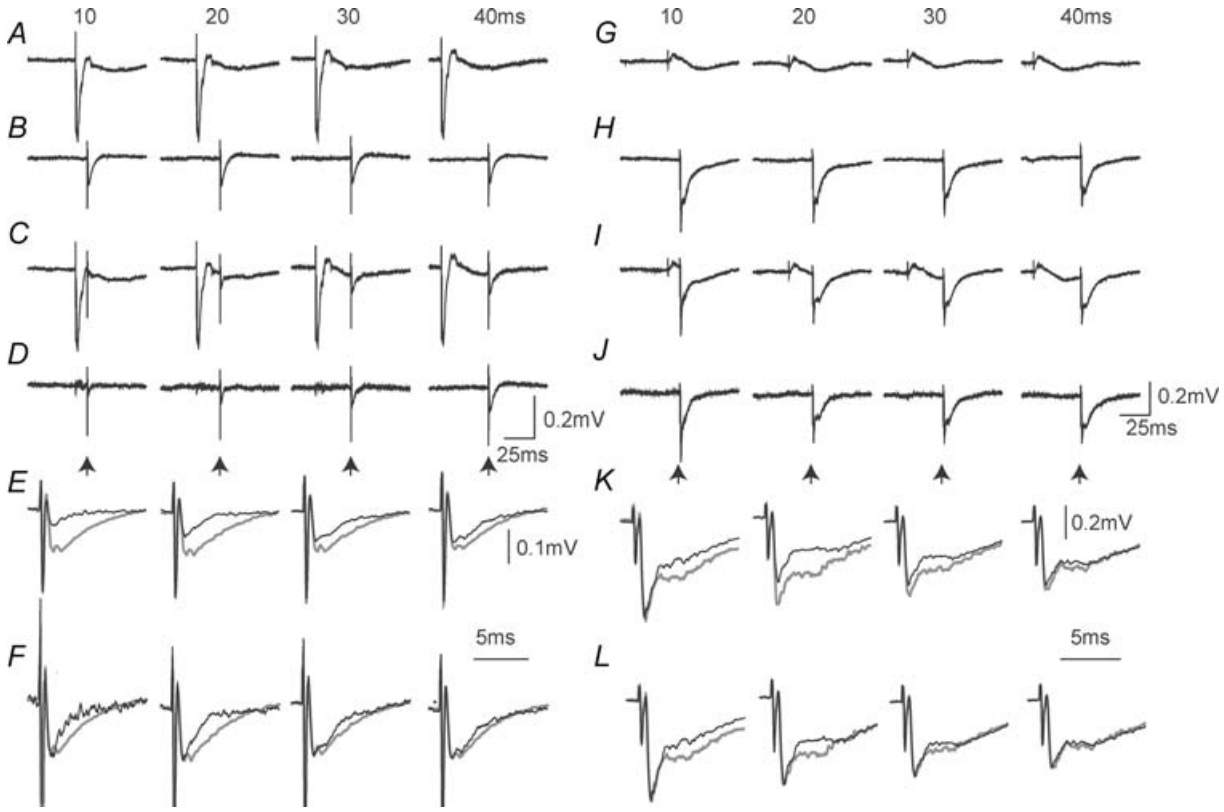

Figure 8. Specimen traces showing the effects of conditioning stimulation on the responses evoked in the dorsal horn of the L2 segment

Test stimuli were delivered to the L2 dorsal root. In *A*–*F*, conditioning stimuli were delivered to the L3 dorsal root (2 mm distant from the recording site) while in *G*–*L*, conditioning stimuli were delivered to the L6 root (8 mm distant). *A* and *G*, the effects of conditioning stimuli delivered alone. *B* and *H*, the control responses. *C* and *I*, the test responses evoked following conditioning stimulation 10–40 ms earlier as indicated. *D* and *J*, the traces formed by subtraction of the responses to conditioning stimulation (i.e. *C*–*A* and *I*–*G*). The traces in *D* and *J* are shown on an expanded time scale in *E* and *K*. In *F* and *L*, the responses have been scaled so that the amplitudes of the synaptic fields of the control and test responses are equal. The full time courses of the effects for these data are illustrated in Fig. 7*D*.

of the fields overlapped and their later phases either overlapped or were parallel indicating a similar time-constant for the decay of both control and test potentials. No signs were apparent of a postsynaptic conduction change that could contribute to the inhibition.

Effects on sural nerve-evoked potentials

The foregoing has shown that stimulation of distant dorsal roots reduces the dorsal horn response to stimulation of the mixed afferents in a nearby dorsal root. It remains to be established whether conditioning stimulation of distant roots inhibits the responses evoked by purely cutaneous afferents. The effects of conditioning stimulation of distant roots on sural nerve-evoked responses were therefore also examined. Field potentials were recorded at depth (400–550 μm) in the dorsal horn of the L5 segment. Typically, the afferent volley could be discriminated and preceded a larger synaptically evoked field. However, the volley was smaller and broader than with dorsal root stimulation and its later part overlapped in time with the onset of the synaptic field. The synaptic field was also broader and had a slower rise-time than with dorsal root stimulation (Fig. 9*A*–*D*).

Figure 9*A*–*D* illustrates the effects of conditioning stimulation of the L6–S3 dorsal roots (100 μA strength) on the field potential evoked by sural nerve stimulation at a variety of C-T stimulus intervals. A potent inhibition of the sural nerve-evoked field potential occurred with simultaneous presentation of stimuli to the L6 dorsal root (with an entry zone 1.5 mm from the recording site) and the sural nerve. This inhibition presumably arose mainly due to an occlusive interaction between the responses to the two stimuli (as it did with dorsal root stimulation; see above). At longer intervals (10–50 ms; Fig. 9*A*), inhibition was still present but could not be explained by occlusion, which was of short duration (see below). Similar, but weaker, long-duration inhibition of the sural nerve-evoked field potentials occurred with conditioning stimulation of the S1 dorsal root (3.5 mm distant), S2 root (6 mm) and S3 root (10 mm). The DRPs evoked by the same stimuli on a dorsal rootlet at L5 level are shown in Fig. 9*E*.

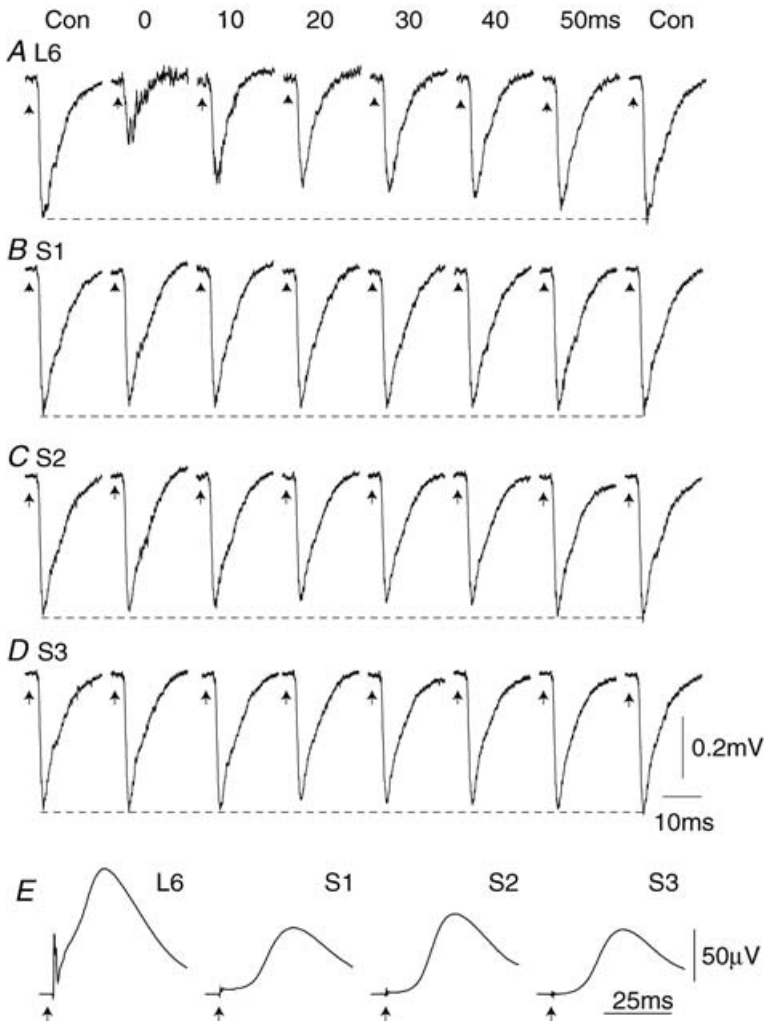

Figure 9. Effects of conditioning stimuli on sural nerve-evoked field potentials in the dorsal horn
A–D averaged synaptic field potentials recorded in the dorsal horn of the L5 spinal segment and evoked by a stimulus of 2 × *T* to the sural nerve. All traces are from a single animal. The responses were conditioned by stimuli of 100 μA to the L6 dorsal root (1.5 mm caudal to the recording electrode) (*A*), S1 (3.5 mm) (*B*), S2 (6 mm) (*C*), or S3 (10 mm) (*D*). The C-T stimulus intervals are shown in *A*. Calibrations in *D* apply throughout *A–D*. The DRPs evoked by the same conditioning stimuli, and recorded simultaneously from a divided rootlet at L5, are shown in *E*.

These effects are quantified in Fig. 10*A* and *B*, which summarizes the data from conditioning stimulation of a total of 30 dorsal roots in 11 preparations. Measurement of an unequivocally monosynaptic component of the evoked fields ($Area_{1ms}$ above) was made difficult because of the temporal spread of the afferent volley and slower rise time of the sural nerve-evoked potentials. Two other measures were therefore used: the area of the first 5 ms of the evoked field ($Area_{5ms}$) and the peak amplitude of the field. Both measures provided qualitatively similar results.

With stimulation of nearby roots (0–3 mm and, to a lesser extent, 3–6 mm distant; Fig. 10*A* and *B*) a powerful early inhibition was apparent in the averaged results. This was present with C-T stimulus intervals of less than 10–12 ms. A second phase of inhibition followed this period, and was apparent also with stimulation of more distant roots (6–9 mm and 9–12 mm; Fig. 10*A* and *B*). The second phase of inhibition was of prolonged duration and peaked at 18–20 ms interstimulus separations for nearby roots and at 20–24 ms for those between 6 and 12 mm distance form the recording site. The potency of the inhibition of sural nerve-evoked field potentials was lower than that seen with dorsal root stimulation: modulation depths measured from the graphs plotted in Fig. 10*B* were 24% (0–3 mm), 9% (3–6 mm), 11% (6–9 mm) and 12% (9–12 mm).

Discussion

The DRPs evoked by stimulation of afferents entering through nearby roots have been the subject of intense study (reviewed in Rudomin *et al.* 1998; Rudomin, 1999; Rudomin & Schmidt, 1999; Willis, 1999). In contrast, the diffuse DRPs evoked over widespread spinal areas

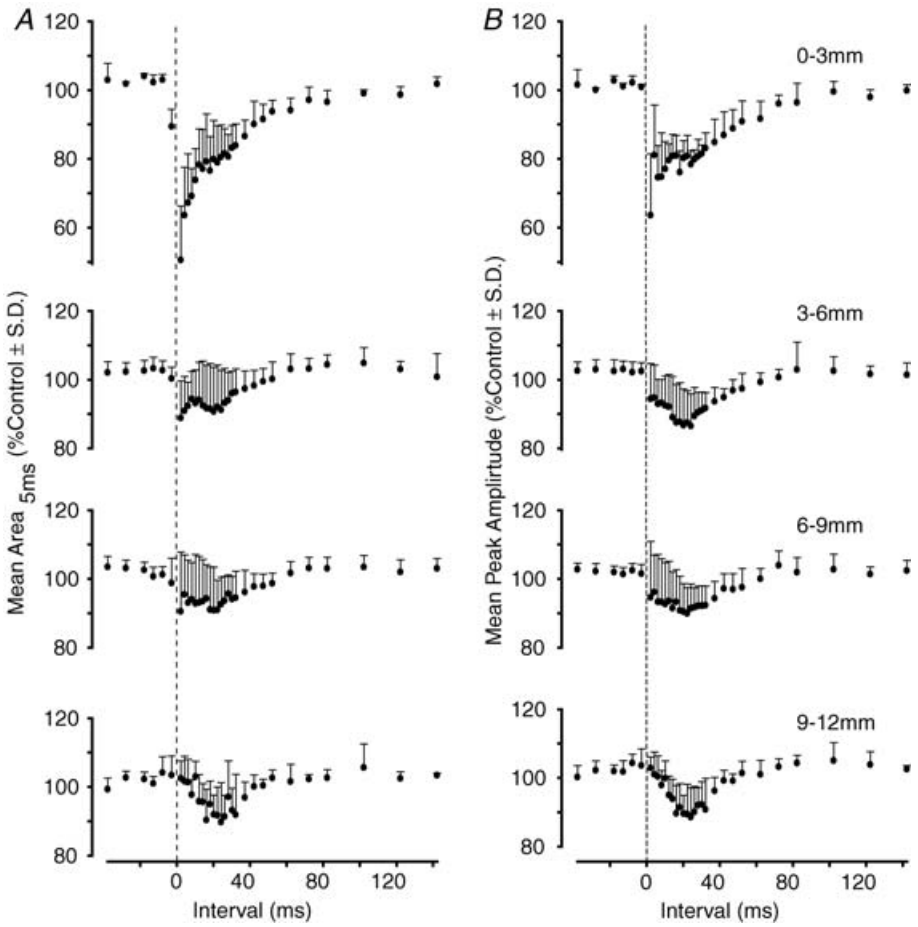

Figure 10. Averaged effects of conditioning stimuli on sural nerve-evoked field potentials in the dorsal horn

In *A* and *B*, the effects of conditioning stimuli for a range of interstimulus intervals, and a range of intersegmental distances, are quantified. *A*, the change in area of the first 5 ms of the evoked field. *B*, the change in peak amplitude. Data were pooled from 11 preparations (0–3 mm, $n = 3$ trials; 3–6 mm, $n = 14$; 6–9 mm, $n = 8$; 9–12 mm, $n = 5$). Interstimulus intervals on the abscissa have been corrected for the additional conduction delay in the sural nerve (2.2 ± 0.13 ms, mean ± S.D., $n = 11$).

have been given little attention although their presence has been noted in both the toad (Dun & Feng, 1944) and the cat (Carpenter *et al.* 1963; Mallart, 1965; Besson & Rivot, 1972; Devor *et al.* 1977; Lupa *et al.* 1979). In addition, Eccles *et al.* (1962*b*) noted that the P-wave of the CDP evoked by group I volleys in muscle nerves could be recorded over several cord segments in the cat. Eccles *et al.* (1962*b*) showed also that PAD of group I muscle afferents monitored directly by intra-axonal recording had a time course that was similar to that of the surface P-wave and to the prolonged negative potentials recorded at depth intraspinally. The time course of PAD also matched that of the increase in excitability of the afferent terminals to electrical stimuli. Similar observations were made in relation to the PAD evoked in large cutaneous afferents (Eccles *et al.* 1963) which were shown to be most strongly depolarized by other cutaneous afferents and more weakly by muscle afferents (Eccles *et al.* 1963; reviewed in Schmidt, 1971). The last-order interneurones mediating PAD in large cutaneous afferents appear to lie in laminae III and IV of the dorsal horn (see Rudomin & Schmidt, 1999 for review).

Relationship to earlier studies

In the present study, long-latency DRPs were observed many segments rostral and caudal to the site of entry of their initiating stimulus (Fig. 2*A* and *B*). They were seen most clearly on roots that were more distant from the stimulus but were also present on nearby roots, although generally masked by the short-latency DRP: in Fig. 9*E* for example, the DRP evoked by L6 stimulation has both short- and long- latency components marked by an inflection on the rising phase. These inflections were seen most clearly when low intensity stimuli were delivered. The locally evoked, short-latency DRPs seen here in the rat appear to correspond to Component I of the DRP reported in the cat by Carpenter *et al.* (1963) while the diffuse DRPs correspond to their Component II. Mallart (1965) described 'heterosegmental' DRPs and equated these with Component II of Carpenter *et al.* (1963). The terms 'local' and 'diffuse' will be used here as they more accurately reflect the spatial distribution of the DRPs.

Association with PAD

The presence of a dorsal root potential provides only equivocal evidence for the presence of an active PAD because the potential may arise passively in the afferents owing to active currents flowing in other spinal elements (see Lloyd, 1952). The present study has provided the first evidence that diffuse DRPs are associated with PAD in the region of the afferent terminals by demonstrating that the DRPs are accompanied by increased electrical excitability of the intraspinal terminals of sural nerve afferents (Figs 5 and 6) and has shown that the DRPs are reduced by the $GABA_A$ antagonist picrotoxin (Fig. 4). While it is possible for changes in excitability to occur without changes in membrane polarization, the circumstances in which this may happen are unlikely to have arisen here (discussed in Wall, 1958; Eccles *et al.* 1962*b*; Burke *et al.* 2001). Given the closely matched time courses of the terminal excitability changes and the DRPs (Fig. 6*A*), it is likely that both arise due to PAD.

The amplitude of the DRP is affected by the distance of the recording electrodes from the terminals and by the size of the recorded roots or rootlets. Measurement of terminal excitability using microstimulation provides a more reliable assay of the changes observed in the terminals within a spatially restricted area of the spinal cord. A further advantage with this method is that PAD of cutaneous A-fibre terminals can be measured in isolation if the volley is recorded from the sural nerve which contains myelinated afferents of exclusively cutaneous origin (Schmalbruch, 1986). The graphs of Fig. 6*C* show that the PAD evoked by distant dorsal root stimulation was potent: the area of the antidromic volley evoked on the sural nerve by an L5 (or L4/5 boundary) test stimulus was increased to 143% of control even with stimulation of roots located 9–12 mm away, i.e. as far caudal as the first coccygeal segment or as far rostral as T11.

Association with presynaptic inhibition

In the present study, electrical stimulation of the mixed afferents in a dorsal root was used to evoke a field potential in the dorsal horn because this method produces a highly synchronized volley and the presynaptic and postsynaptic potentials are clearly separated in time (Fig. 7*C*). During the fast rising phase of an excitatory postsynaptic potential, the majority of membrane current (I_m) will be carried through the membrane capacitance (C_m). The amplitude of the extracellular potential (V_{ext}) will therefore be approximately proportional to these currents, i.e.

$$V_{ext} \propto I_m \approx C_m(dV_m/dt)$$

where V_m is the membrane potential (see Johnston & Wu, 1995). The reduction in the peak negativity of the synaptic fields with conditioning stimuli of both nearby and distant dorsal roots (Figs 7*B* and 8*E* and *K*) therefore indicates a reduction in the peak currents evoked by the test stimuli. The early part of the postsynaptic field potential, up to 1 ms after the peak of the afferent volley ($Area_{1ms}$ in Fig. 7*D* and *F*), reflects activity at the first central synapse as there is insufficient time for disynaptic or longer pathways to contribute. A reduction in this area therefore indicates inhibition at the site of the primary afferent synapse onto second-order spinal neurones. As the extracellular potential amplitude is proportional to synaptic current,

this area provides an estimate of the relative charge transfer during the first 1 ms of the monosynaptically evoked EPSP. Figure 7*D* shows clear inhibition that has a time course that closely matches that of the dorsal root potential. The inhibition is quantified further in Fig. 7*E* and *F*. In Fig. 7*F*, inhibition was clearly present even when conditioning stimuli were delivered to the roots of segments 12 mm or more from the recording point (an average of 7.5 spinal segments; range 6–9, $n = 6$).

Even with intracellular recordings of EPSPs, it can be difficult to differentiate between pre- and postsynaptic inhibitory mechanisms (reviewed by Burke & Rudomin, 1977). Matters are complicated further as presynaptic and postsynaptic inhibition may be evoked together (see, e.g. Rudomin & Schmidt, 1999). With conditioning stimulation of distant roots, the time course of the declining phase of the evoked fields was unaltered (Figs 7*B* and 8*L*). Thus, there were no signs of a postsynaptic conductance change and the inhibition may be exclusively presynaptic in origin although other methods will be needed to establish this unequivocally. With stimulation of nearby roots (e.g. Fig. 8*F*), mixed pre- and postsynaptic effects may contribute to the evoked inhibition.

The data shown in Figs 9 and 10 confirm that inhibition of the responses evoked by cutaneous afferents was seen with stimulation of both nearby and distant dorsal roots. The results were similar to those obtained with dorsal root stimulation (Fig. 7). A long-lasting inhibition was evoked (Fig. 9*A*–*D*) with a duration that closely matched the DRP (Fig. 9*E*). The potency of the inhibition evoked by stimulation of distant dorsal roots (Fig. 10*A* and *B*) was less than that observed with dorsal root stimulation (Fig. 7*F*) but it should be noted that $\text{Area}_{5\text{ms}}$ measurements of the sural nerve field potentials will have included contributions from di- and poly-synaptic pathways.

Underlying mechanisms

It was not the purpose of the present study to examine the details of the mechanisms underlying the diffuse DRPs but several observations are relevant to these. While both local and diffuse DRPs were present in preparations with intact neuraxes (Fig. 1*C*), the majority of the present experiments were done in animals with the spinal cord transected at mid-thoracic level. The long-latency DRPs must therefore depend upon intrinsic spinal circuits for their generation; they cannot depend upon long-loop pathways through higher centres. In this respect, the mechanisms described here are distinct form those of diffuse noxious inhibitory control described by Le Bars *et al.* (1979*a*,*b*)

The effects on the DRP of the GABA_A antagonist picrotoxin were examined. Note that picrotoxin, unlike strychnine, does not appear to augment oscillatory activity in DRP-generating circuits even at the convulsant doses used here (Lidierth, 2004; Lidierth & Wall, 1997). The DRPs evoked by stimulation of nearby and distant roots were both dose-dependently reduced by administration of picrotoxin (Fig. 4). However, they were not abolished, suggesting that both include a non-GABA_A receptor mediated component although this was small ($< 17\%$). Similar observations have been made elsewhere for the DRPs evoked on nearby roots (e.g. Thompson & Wall, 1996; Kremer & Lev-Tov, 1998; Russo *et al.* 2000; Lee *et al.* 2002). It appears therefore that both local and diffuse DRPs are mediated primarily by GABAergic last-order interneurones. It remains to be seen whether a common population of last-order interneurones mediate both types of response.

The propagation of the afferent volley in the dorsal columns occurred with constant conduction velocity (Fig. 2). The sharp discontinuity in the latency-to-onset of the DRPs cannot therefore be explained by conduction delays in the dorsal columns. On entering the spinal cord, primary afferents bifurcate and provide collateral projections to neighbouring and more distant segments (Wilson & Kitchener, 1996). Spread of the local DRPs probably depends largely on the spread of excitation in the dorsal columns (see below). Primary afferents also contribute approximately two-thirds of the fibres in the Lissauer tract of the rat and, in the lumbosacral cord, these can have a rostro-caudal extent of several segments (Chung *et al.* 1979). They might therefore contribute to the spread of excitation generating the local DRPs reported here. While primary afferents terminate in segments that are distant from their point of entry to the cord, the more distant terminals appear to be weak or ineffective at least under normal physiological conditions (Wall, 1995; Wilson & Kitchener, 1996). Transient increases in the efficacy of the distant terminals may account for the observation that short latency DRPs were occasionally seen at long distances (as in Fig. 2*B*).

In the toad, a late component of the distantly evoked DRP survives lesions of the dorsal columns between the stimulus and recording point while an earlier component does not (Dun & Feng, 1944). In the cat, Wall (1962) and Cervero *et al.* (1978) observed that a lesion of the dorsal columns between stimulated and recorded adjacent dorsal roots caused a prolongation in the latency-to-onset of the DRP. These observations suggest that the local, short-latency DRPs are evoked in immediately neighbouring segments via the effects of primary afferents in the dorsal columns and that abolition of the local DRPs by the dorsal column lesion unmasks a longer latency DRP with an intersegmental spread that is independent of the dorsal columns. The late-component of the DRP together with those DRPs evoked in distant segments appear to depend on propriospinal systems which may include the Lissauer tract (Wall, 1962), dorsolateral funiculus (Cervero *et al.* 1978) and lateral funiculus (Bayev & Kostyuk, 1981).

Using intraspinal microstimulation of the dorsal columns in the cat, Harrison & Jankowska (1984) also evoked short-latency intersegmental DRPs that were converted to a longer latency-to-onset by dorsal column lesions. Similar long-latency DRPs were evoked by microstimulation in the superficial dorsal horn and these were unaffected by dorsal column lesions (Harrison & Jankowska, 1984). The superficial dorsal horn is a source of cells that project intersegmentally via the Lissauer tract (Szentagothai, 1964) and low-strength microstimulation of this tract has been shown to evoke long-latency DRPs in the absence of any signs of activation of primary afferent fibres (Wall & Yaksh, 1978; Lidierth & Wall, 1998; Wall *et al.* 1999). As the majority of propriospinal axons in the tract of Lissauer do not project beyond their segment of origin (Cervero *et al.* 1979), their involvement in mediating the diffuse DRPs would appear to require the activation of a rostro-caudally directed chain of propriospinal interneurones.

Functional significance

The diffuse DRPs are not an artefact of electrical stimulation as they are present with natural stimulation such as a brief non-noxious paw-tap (Fig. 3). They exhibit a very low threshold to such stimuli (< 1 gram force) which suggests that diffuse DRPs will be evoked during normal behaviour and evoke presynaptic inhibition. The diffuse mechanisms may contribute to movement-related modulation of PAD which plays an important role in modulating sensory transmission during movement (see also Beloozerova & Rossignol, 1999, 2004; Menard *et al.* 1999, 2002; Cote & Gossard, 2003; Seki *et al.* 2003 reviewed in Rudomin & Schmidt, 1999.) Supraspinal control of PAD circuits appears to contribute to anticipatory (feed-forward) adjustments of sensory transmission (Seki *et al.* 2003). The present paper has not examined descending control of the diffuse mechanisms directly but it is noteworthy that neurones that are excited by stimulation of the Lissauer tract, which are candidate neurones to mediate the diffuse DRPs, respond to stimulation of the sensorimotor cortex as well as to both low-threshold muscle and cutaneous afferents (Wall & Lidierth, 1997; Lidierth & Wall, 1998). These cells also respond vigorously to light mechanical stimulation (Wall *et al.* 1999).

This study has concentrated on PAD evoked in terminals close to their point of entry in the spinal cord. PAD in more distant terminals which are subjected to presynaptic inhibition (reviewed in Wall, 1995) have thus far not been examined. However, the diffuse PAD-generating circuit would appear to be well-suited to regulation of these widespread collaterals and thus to the functional regulation of the dermatomal organization of the spinal cord (e.g. Denny-Brown *et al.* 1973; Greenberg, 2003).

The presence of parallel pathways mediating PAD in the toad (Dun & Feng, 1944), the cat (Carpenter *et al.* 1963; Mallart, 1965; Devor *et al.* 1977) and now the rat suggests that this is a fundamental feature of the organization of PAD-generating spinal circuits. However, it is a feature that has received little detailed attention. The demonstration here that the diffuse DRPs are robustly evoked by weak natural stimuli, produce potent changes in terminal excitability, and evoke inhibition that is at least partly presynaptic suggests that greater attention should be given to discriminating the roles of the local and diffuse networks in future work on PAD.

References

Barron DH & Matthews BHC (1938). The interpretation of potential changes in the spinal cord. *J Physiol* **92**, 276–321.

Bayev KV & Kostyuk PG (1981). Primary afferent depolarization evoked by the activity of spinal scratching generator. *Neuroscience* **6**, 205–215.

Beloozerova I & Rossignol S (1999). Antidromic discharges in dorsal roots of decerebrate cats – I. Studies at rest and during fictive locomotion. *Brain Res* **846**, 87–105.

Beloozerova IN & Rossignol S (2004). Antidromic discharges in dorsal roots of decerebrate cats. II: studies during treadmill locomotion. *Brain Res* **996**, 227–236.

Besson JM & Rivot JP (1972). Heterosegmental, heterosensory and cortical inhibitory effects on dorsal interneurones in the cat's spinal cord. *Electroencephalogr Clin Neurophysiol* **33**, 195–206.

Burke D, Kiernan MC & Bostock H (2001). Excitability of human axons. *Clin Neurophysiol* **112**, 1575–1585.

Burke RE & Rudomin P (1977). Spinal neurons and synapses. *Handbook of Physiology*, section 1, *The Nervous System*, vol. I, *Cellular Biology of Neurons*, ed. Brookhart JM & Mountcastle VB, Kandel ER & Geiger SR, pp. 877–944. American Physiological Society, Bethesda.

Carpenter D, Engberg I, Funkenstein H & Lundberg A (1963). Decerebrate control of reflexes to primary afferents. *Acta Physiol Scand* **59**, 424–437.

Cervero F, Iggo A & Molony V (1978). The tract of Lissauer and the dorsal root potential. *J Physiol* **282**, 295–305.

Cervero F, Iggo A & Molony V (1979). segmental and intersegmental organization of neurons in the substantia gelatinosa rolandi of the cats spinal-cord. *Q J Exp Physiol Cognate Med Sciences* **64**, 315–326.

Chung K, Langford LA, Applebaum AE & Coggeshall RE (1979). Primary afferent fibers in the tract of Lissauer in the rat. *J Comp Neurol* **184**, 587–598.

Cote MP & Gossard JP (2003). Task-dependent presynaptic inhibition. *J Neurosci* **23**, 1886–1893.

Denny-Brown D, Kirk EJ & Yanagisawa N (1973). The tract of Lissauer in relation to sensory transmission in the dorsal horn of spinal cord in the macaque monkey. *J Comp Neurol* **151**, 175–200.

Devor M, Merrill EG & Wall PD (1977). Dorsal horn cells that respond to stimulation of distant dorsal roots. *J Physiol* **270**, 519–531.

Dun FT & Feng TP (1944). A note on the two components of the dorsal root potential. *J Neurophysiol* **7**, 327–329.

Eccles JC, Kostyuk PG & Schmidt RF (1962*a*). Central pathways responsible for depolarization of primary afferent fibres. *J Physiol* **161**, 237–257.

Eccles JC, Magni F & Willis WD (1962*b*). Depolarization of central terminals of group I afferent fibres from muscle. *J Physiol* **160**, 62–93.

Eccles JC, Schmidt RF & Willis WD (1963). Depolarization of the central terminals of cutaneous afferent fibers. *J Neurophysiol* **26**, 646–661.

Eguibar JR, Quevedo J, Jimenez I & Rudomin P (1994). Selective cortical control of information-flow through different intraspinal collaterals of the same muscle afferent fiber. *Brain Res* **643**, 328–333.

Eguibar JR, Quevedo J & Rudomin P (1997). Selective cortical and segmental control of primary afferent depolarization of single muscle afferents in the cat spinal cord. *Exp Brain Res* **113**, 411–430.

Greenberg SA (2003). The history of dermatome mapping. *Arch Neurol* **60**, 126–131.

Harrison PJ & Jankowska E (1984). Do interneurones in lower lumbar segments contribute to the presynaptic depolarization of group I muscle afferents in Clarke's column? *Brain Res* **295**, 203–210.

Jankowska E, Bichler E & Hammar I (2000). Areas of operation of interneurons mediating presynaptic inhibition in sacral spinal segments. *Exp Brain Res* **133**, 402–406.

Johnston DA & Wu SM-S (1995). *Fundamentals of Cellular Neurophysiology*. MIT Press, Cambridge, Massachusetts.

Kremer E & Lev-Tov A (1998). GABA-receptor-independent dorsal root afferents depolarization in the neonatal rat spinal cord. *J Neurophysiol* **79**, 2581–2592.

Le Bars D, Dickenson AH & Besson JM (1979*a*). Diffuse noxious inhibitory controls (DNIC). I. Effects on dorsal horn convergent neurones in the rat. *Pain* **6**, 283–304.

Le Bars D, Dickenson AH & Besson JM (1979*b*). Diffuse noxious inhibitory controls (DNIC). II. Lack of effect on non-convergent neurones, supraspinal involvement and theoretical implications. *Pain* **6**, 305–327.

Lee CJ, Bardoni R, Tong CK, Engelman HS, Joseph DJ, Magherini PC & MacDermott AB (2002). Functional expression of AMPA receptors on central terminals of rat dorsal root ganglion neurons and presynaptic inhibition of glutamate release. *Neuron* **35**, 135–146.

Lidierth M (2004). Strychnine-sensitive mechanisms regulating primary afferent depolarization in the rat spinal cord. *J Physiol* **565.P**, C111.

Lidierth M (2005*a*). Dorsal root potentials and intersegmental inhibition in the rat spinal cord. *J Physiol* **567.P**, C107.

Lidierth M (2005*b*). Pulser: user-friendly, graphical user interface based software for controlling stimuli during data acquisition with Spike2 for Windows. *J Neurosci Meth* **141**, 243–250.

Lidierth M & Wall PD (1996). Synchronous inherent oscillations of potentials within the rat lumbar spinal cord. *Neurosci Lett* **220**, 25–28.

Lidierth M & Wall PD (1997). The effects of picrotoxin on the spontaneous dorsal root potentials in the spinalized rat. *J Physiol* **501.P**, 46–47.

Lidierth M & Wall PD (1998). Dorsal horn cells connected to the Lissauer tract and their relation to the dorsal root potential in the rat. *J Neurophysiol* **80**, 667–679.

Lidierth M & Wall PD (2001). Short- and long-latency dorsal root potentials in rat spinal cord. *J Physiol* **531.P**, 136*P*.

Lloyd DPC (1952). Electrotonus in dorsal root nerves. *Cold Spring Harb Symp Quant Biol* **17**, 203–219.

Lloyd DPC & McIntyre AK (1949). On the origins of dorsal root potentials. *J General Physiol* **32**, 409–443.

Lomeli J, Castillo L, Linares P & Rudomin P (2000). Effects of PAD on conduction of action potentials within segmental and ascending branches of single muscle afferents in the cat spinal cord. *Exp Brain Res* **135**, 204–214.

Lomeli J, Quevedo J, Linares P & Rudomin P (1998). Local control of information flow in segmental and ascending collaterals of single afferents. *Nature* **395**, 600–604.

Lupa K, Wojcik G, Ozog M & Niechaj A (1979). Spread of the dorsal root potentials in lower lumbar, sacral and upper caudal spinal cord. *Pflugers Arch* **381**, 201–207.

Mallart A (1965). Heterosegmental and heterosensory presynaptic inhibition. *Nature* **206**, 719–720.

Manjarrez E, Jimenez I & Rudomin P (2003). Intersegmental synchronization of spontaneous activity of dorsal horn neurons in the cat spinal cord. *Exp Brain Res* **148**, 401–413.

Manjarrez E, Rojas-Piloni JG, Jimenez I & Rudomin P (2000). Modulation of synaptic transmission from segmental afferents by spontaneous activity of dorsal horn spinal neurones in the cat. *J Physiol* **529**, 445–460.

Menard A, Leblond H & Gossard JP (1999). The modulation of presynaptic inhibition in single muscle primary afferents during fictive locomotion in the cat. *J Neurosci* **19**, 391–400.

Menard A, Leblond H & Gossard JP (2002). Sensory integration in presynaptic inhibitory pathways during fictive locomotion in the cat. *J Neurophysiol* **88**, 163–171.

Rudomin P (1999). Presynaptic selection of afferent inflow in the spinal cord. *J Physiol Paris* **93**, 329–347.

Rudomin P, Romo R & Mendell L (1998). *Presynaptic Inhibition and Neural Control*. Oxford University Press, New York.

Rudomin P & Schmidt RF (1999). Presynaptic inhibition in the vertebrate spinal cord revisited. *Exp Brain Res* **129**, 1–37.

Russo RE, Delgado-Lezama R & Hounsgaard J (2000). Dorsal root potential produced by a TTX-insensitive micro-circuitry in the turtle spinal cord. *J Physiol* **528**, 115–122.

Schmalbruch H (1986). Fiber composition of the rat sciatic nerve. *Anat Rec* **215**, 71–81.

Schmidt RF (1971). Presynaptic inhibition in vertebrate central nervous system. *Ergebnisse Physiologie Biologischen Chemie Experimentellen Pharmakologie* **63**, 20–101.

Seki K, Perlmutter SI & Fetz EE (2003). Sensory input to primate spinal cord is presynaptically inhibited during voluntary movement. *Nat Neurosci* **6**, 1309–1316.

Szentagothai J (1964). Neuronal and synaptic arrangement in the substantia gelatinosa Rolandi. *J Comp Neurol* **122**, 219–239.

Thompson SW & Wall PD (1996). The effect of GABA and 5-HT receptor antagonists on rat dorsal root potentials. *Neurosci Lett* **217**, 153–156.

Wall PD (1958). Excitability changes in afferent fiber terminations and their relation to slow potentials. *J Physiol* **142**, 1–21.

Wall PD (1962). Origin of a spinal-cord slow potential. *J Physiol* **164**, 508–&.
Wall PD (1995). Do nerve impulses penetrate terminal arborizations – a pre-presynaptic control mechanism. *Trends Neurosci* **18**, 99–103.
Wall PD & Lidierth M (1997). Five sources of a dorsal root potential: Their interactions and origins in the superficial dorsal horn. *J Neurophysiol* **78**, 860–871.
Wall PD, Lidierth M & Hillman P (1999). Brief and prolonged effects of Lissauer tract stimulation on dorsal horn cells. *Pain* **83**, 579–589.
Wall PD & Yaksh TL (1978). Effect of Lissauer tract stimulation on activity in dorsal roots and in ventral roots. *Exp Neurol* **60**, 570–583.
Whitehorn D & Burgess PR (1973). Changes in polarization of central branches of myelinated mechanoreceptor and nociceptor fibers during noxious and innocuous stimulation of the skin. *J Neurophysiol* **36**, 226–237.
Willis WD (1999). Dorsal root potentials and dorsal root reflexes: a double-edged sword. *Exp Brain Res* **124**, 395–421.
Wilson P & Kitchener PD (1996). Plasticity of cutaneous primary afferent projections to the spinal dorsal horn. *Prog Neurobiol* **48**, 105–129.

Acknowledgements

I am greatly indebted to the late Professor Patrick D. Wall who took part in some of the early experiments in this study and provided much helpful advice. Professor Thomas A. Sears kindly provided comments on the manuscript. This work was supported by the Wellcome Trust (grant no. 052639).